Disturbance rejection using the combination of equivalent-input-disturbance and model-predictive-control methods

Kou Miyamoto*, Yuta Tomiyoshi*, Naoto Yoshida*, Satoshi Nakano†, Jinhua She‡
* Institute of Technology, Shimizu Corporation, Tokyo, Japan
† Dept. of Engineering, Nagoya Institute of Technology, Nagoya, Japan
‡ School of Engineering, Tokyo University of Technology, Hachioji, Tokyo 192-0982, Japan
E-mails: {kou_miyamoto, y.tomiyoshi0423, n.yoshida}@shimz.co.jp, nakano@nitech.ac.jp, she@stf.teu.ac.jp

IECON 2023- 49th Annual Conference of the IEEE Industrial Electronics Society | 979-8-3503-3182-0/23/$31.00 ©2023 IEEE | DOI: 10.1109/IECON51785.2023.10312146

Abstract—This paper presents a new equivalent-input-disturbance (EID) approach that is the combination of the EID approach and model-predictive-control (MPC) method. The EID approach estimates the influence of a disturbance and uses it to reject the disturbance. Thus, the amplitude of the control input can be beyond the limitation if the original disturbance is large. To solve this problem, this paper combines the EID approach and the MPC method. The MPC method adjusts the amplitude of an estimated EID during a large disturbance. A numerical example uses a structural model and an earthquake. The results of it verify the validity of our method and the presented method has a better control performance than the previous EID approach. Furthermore, the MPC method adjusts the control input lest it is beyond the limitation.

Index Terms—Equivalent-input-disturbance approach, Model predictive control, Disturbance rejection, Active control, Disturbance rejection.

I. Introduction

An active-disturbance-rejection strategy is one of the key strategies to improving control performance. This method estimates a disturbance and uses it to reject it. One of the most common methods is the equivalent input disturbance approach (EID), which is devised by She et al. [1], and has been applied in many fields such as active structural control [2], [3], drilling trajectory [4], and smart grid [5]. The EID approach estimates the signal, the response of which is the same as that of the original disturbance. Usually, the control and disturbance input channels are not the same; estimating an EID signal but not the original disturbance is more effective to reject the disturbance. In other words, the EID approach is useful for an unmatched disturbance. Thus, the EID approach can be used for many systems and this is one of the advantages of the approach.

However, if the amplitude of the original disturbance is large, then it results in saturation of the control input and may decrease the control performance. Miyamoto et al. showed that the amplitude of an estimated EID can be adjusted by tuning the low-pass filter that is used to calculate an EID signal [3]. Thus, if the amplitude of a disturbance is expected to be large, then adjusting the low-pass filter prevents saturating the control input. However, this low-pass filter decreases the control performance for small disturbances.

In recently, the model-predictive-control (MPC) method [6] has been used to deal with constraints [7], [8]. The MPC method estimates future responses and solves an optimization problem with constraints in every time step. One of the advantages of the MPC method makes it easy to handle a system with constraints.

This paper presents the MPC-based EID approach that combines the EID approach and the MPC method to take into account the limitation of the control input. The numerical verification showed that the maximum control input satisfies the limitation, and the presented system has better control performance than a previous EID system.

II. EID approach

This section explains the concept of the EID approach. Consider the following system:

$$\begin{cases} x[k+1] = Ax[k] + B_u u[k] + B_d d[k] \\ y[k] = Cx[k] \end{cases} \tag{1}$$

where A is the system matrix, B_u is the control-input matrix, B_d is the disturbance-input matrix, C is the output matrix, $x[k]$ is the state of the system, $y[k]$ is the output, $d[k]$ is the disturbance, and $u[k]$ is the control input. Without loss of generality, we assume that $(A,\, B_u)$ is controllable and $(A,\, C)$ is observable. Next, we consider the following system, the disturbance of which $d_e[k]$ inputs to the control input channel B_u:

$$\begin{cases} \bar{x}[k+1] = A\bar{x}[k] + B_u[u[k] + d_e[k]] \\ \bar{y}[k] = C\bar{x}[k] \end{cases} \tag{2}$$

where $\bar{x}[k]$ is the response for the disturbance $d_e[k]$. For the systems (1) and (2), if $y[k] = \bar{y}[k]$, then the disturbance $d_e[k]$ is defined as an EID of the original disturbance $d[k]$. The previous studies focused on the way to estimate the EID.

Next, we explain the estimation process of an EID. The estimation system is shown in Fig. 1. Figure 1 shows

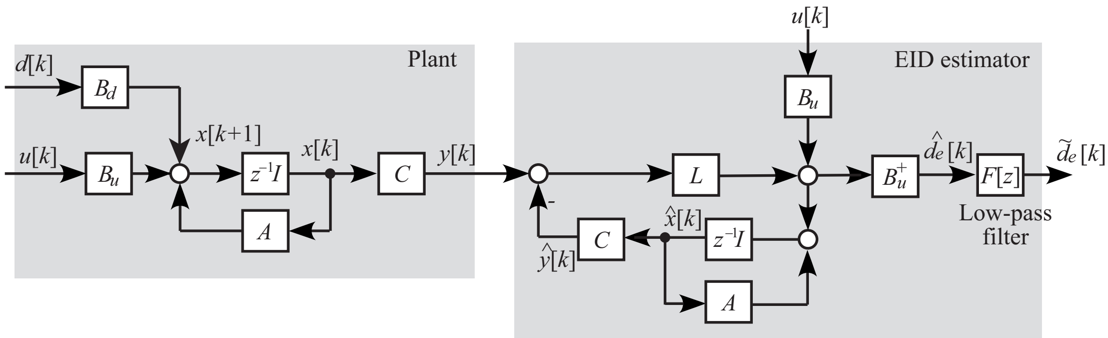

Fig. 1. EID estimation system.

that the estimation system has a state observer with an observer gain L, a low-pass filter $F[z]$, and the pseudo inverse matrix of the control input matrix (B_u) B_u^+:

$$B_u^+ = (B_u^{\mathrm{T}} B_u)^{-1} B_u^{\mathrm{T}}. \tag{3}$$

The low-pass filter is selected to be

$$\begin{cases} F[z] = \dfrac{\beta}{z+\alpha}, \\ \alpha = \mathrm{e}^{-T_s/T},\ \beta = 1 - \mathrm{e}^{T_s/T} \end{cases} \tag{4}$$

where T_s is a sampling period and T is the time constant of the filter, which determines the cut-off frequency of the filter.

The observer is described as follows:

$$\begin{cases} \hat{x}[k+1] = (A - LC)\hat{x}[k] + B_u u[k] + Ly[k], \\ \hat{y}[k] = C\hat{x}[k] \end{cases} \tag{5}$$

where $\hat{x}[k]$ is the estimated $x[k]$. Equations (2) and (5) yield

$$\Delta x[k+1] = (A - LC)\Delta x[k] + B_u d_e[k]. \tag{6}$$

Since we assumed (A, B_u) is controllable, then there exits $\Delta d[k]$ that satisfies

$$\Delta x[k+1] = A\Delta x[k] + B_u \Delta d[k]. \tag{7}$$

Equations (5) and (7) obtain the estimated EID $\hat{d}_e[k]$ as follows

$$\begin{cases} \hat{d}_e[k] = B_u^+ LC\Delta x[k], \\ \hat{d}_e[k] = d_e[k] - \Delta d[k] \end{cases} \tag{8}$$

where $\hat{d}_e[k]$ is the estimated EID. Equation (8) shows that if the state observer has a good estimation performance, which means that $\Delta x[k]$ is small; then it reduces the estimation error for the EID $\Delta d[k]$. We use a low-pass filter to reduce the influence of the estimation error $\Delta d[k]$. The estimated EID with a low-pass filter $\tilde{d}_e[k]$ is

$$\tilde{D}_e[z] = F[z]\hat{D}_e[z] \tag{9}$$

where $\tilde{D}_e[z]$ and $\hat{D}_e[z]$ are the z-transformed $\tilde{d}_e[k]$ and $\hat{d}_e[k]$.

III. MPC method

This section first explains the MPC method. Then, we explain the combination of the MPC and EID methods.

This section explain the MPC method and the control input $u(t)$ is assumed that $u[k] = u_{\mathrm{mpc}}[k]$, where $u_{\mathrm{mpc}}[k]$ is the control input of the MPC. Consider the control system (1) with $u[k] = u_{\mathrm{mpc}}[k]$:

$$\begin{cases} x[k+1] = Ax[k] + Bv[k], \\ y[k] = Cx[k], \\ B = \begin{bmatrix} B_u & B_d \end{bmatrix},\quad v^{\mathrm{T}}[k] = \begin{bmatrix} u_{\mathrm{mpc}}^{\mathrm{T}}[k] & d^{\mathrm{T}}[k] \end{bmatrix}. \end{cases} \tag{10}$$

The predicted states can be represented as follows:

$$\begin{cases} x[k+1|k] = Ax[k] + Bv[k], \\ x[k+2|k] = A^2 x[k] + ABv[k] + Bv[k+1|k], \\ \qquad \vdots \\ x[k+h_p|k] = A^{h_p} x[k] + A^{h_p-1} Bv[k] \ldots \\ \qquad + A^{h_p-2} Bv[k+1|k] + A^{h_p-h_v} Bv[k+h_v-1|k] \end{cases} \tag{11}$$

where $x[k+i|k]$ indicates the predicted state at $k+i$ with the current state $x[k]$, h_p is the prediction horizon and h_v is the input horizon.

Define the vector for the predicted states and inputs:

$$\begin{cases} X[k] = \begin{bmatrix} x^{\mathrm{T}}[k] & x^{\mathrm{T}}[k+1|k] & \cdots & x^{\mathrm{T}}[k+h_p|k] \end{bmatrix}^{\mathrm{T}}, \\ V[k] = \begin{bmatrix} v^{\mathrm{T}}[k] & v^{\mathrm{T}}[k+1|k] & \cdots & v^{\mathrm{T}}[k+h_p|k] \end{bmatrix}^{\mathrm{T}}. \end{cases} \tag{12}$$

Therefore, the predicted output $Y[k]$ is given as follows:

$$Y[k] = \Psi X[k] + \Theta V[k] \tag{13}$$

where

$$\begin{cases} \Psi = \begin{bmatrix} CA & CA^2 & \cdots & CA^{h_p} \end{bmatrix}^{\mathrm{T}}, \\ \Theta = \begin{bmatrix} CB & 0 & \cdots & 0 \\ CAB & CB & \cdots & 0 \\ CA^2B & CAB & \cdots & 0 \\ \vdots & \vdots & \vdots & \vdots \\ CA^{h_p-1}B & CA^{h_p-2}B & \cdots & CA^{h_p-h_v}B \end{bmatrix}. \end{cases} \tag{14}$$

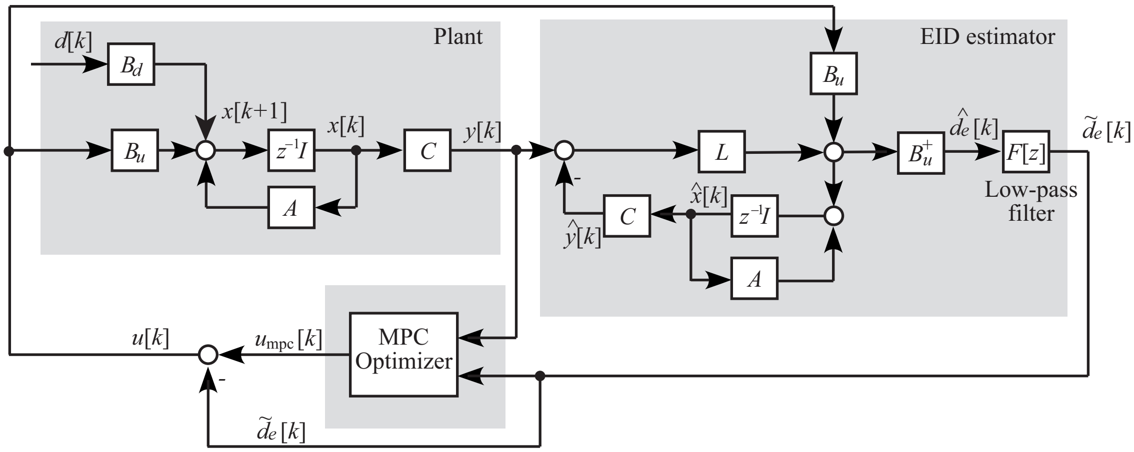

Fig. 2. Block diagram of MPC-based EID approach system

The control input of the MPC $u_{\mathrm{mpc}}[k]$ is yielded by minimizing the following cost function $J[k]$:

$$\begin{cases} J[k] = Y^{\mathrm{T}}[k]QY[k] + U_{\mathrm{mpc}}^{\mathrm{T}}[k]RU_{\mathrm{mpc}}[k], \\ U_{\mathrm{mpc}}[k] = \begin{bmatrix} u_{\mathrm{mpc}}^{\mathrm{T}}[k] & \cdots & u_{\mathrm{mpc}}^{\mathrm{T}}[k+h_p|k] \end{bmatrix}^{\mathrm{T}}. \end{cases} \tag{15}$$

where Q (> 0) and R (> 0) are the weighting matrices for $Y[k]$ and $u_{\mathrm{mpc}}[k]$, respectively. Note that this paper uses both the MPC method and the EID approach. The next section explains how to combine these methods.

IV. MPC-based EID approach

This paper presents the MPC-based EID approach that combines the EID approach and the MPC method. The control system has two kinds of control input, namely the estimated EID $\tilde{d}_e[k]$ and the control input of the MPC $u_{\mathrm{mpc}}[k]$. If we consider the limitation of a control input $u_{\max}$, then the cost function (15) is minimized with the constraint:

$$|-\tilde{d}_e[k] + u_{\mathrm{mpc}}[k]| \leq u_{\max}. \tag{16}$$

The algorithm for calculating the control input at $k-$step is as follows:

Step 1 : Obtain the value $y[k]$.
Step 2 : Calculate an estimated EID $\tilde{d}_e[k]$.
Step 3 : Set the constraint (16) using $\tilde{d}_e[k]$ obtained in Step 2.
Step 4 : Solve the optimization problem for the objective function (15) with the output $y[k]$ and the constraint (16), which is defined in Step 3. Then, the control input of the MPC $u_{\mathrm{mpc}}[k]$ is obtained.
Step 5 : The total control input $u[k]$ is calculated by $u[k] = -\tilde{d}_e[k] + u_{\mathrm{mpc}}[k]$.

The control system is shown in Fig. 2.

V. Numerical example

This section verifies our method with a numerical example. We use a structural model with a Kobe wave, which is one of the most common wave. The dynamics of a structure is

$$M_S\ddot{x}_S(t) + C_S\dot{x}_S(t) + K_Sx_S(t) = -M_S\ddot{x}_g(t) + u(t) \tag{17}$$

where M_S, C_S, and K_S are the mass, damping coefficient, and the stiffness of the structure; and $x_S(t)$ and $\ddot{x}_g(t)$ are the displacement of the structure and the ground acceleration. The parameters of the structure, M_S, K_S, and C_S, are 4.0×10^6 kg, 1.58×10^8 N/m, and 1.01×10^6 Ns/m, respectively.

The state space representation of the structural model is as follows:

$$\underbrace{\begin{bmatrix} \dot{x}_S(t) \\ \ddot{x}_S(t) \end{bmatrix}}_{\dot{x}_c(t)} = \underbrace{\begin{bmatrix} 0 & 1 \\ -\frac{K_S}{M_S} & -\frac{C_S}{M_S} \end{bmatrix}}_{A_c} \underbrace{\begin{bmatrix} x_S(t) \\ \dot{x}_S(t) \end{bmatrix}}_{x_c(t)} + \underbrace{\begin{bmatrix} 0 \\ \frac{1}{M_S} \end{bmatrix}}_{B_u} u(t) + \underbrace{\begin{bmatrix} 0 \\ -1 \end{bmatrix}}_{B_d} \ddot{x}_g(t). \tag{18}$$

The zero-order-hold method with a sampling time 0.01 s ($T_s = 0.01$) is used to make the discrete model.

The accelerogram and the Fourier spectrum of the Kobe wave are shown in Fig. 3.

For the design of the control system, the parameters are selected as follows:

$$\begin{cases} Q = \begin{bmatrix} 10^{30} & 0 \\ 0 & 10 \end{bmatrix}, \quad R = 0.001, \\ T = 0.01, \quad h_p = 20, \quad h_v = 1. \end{cases} \tag{19}$$

Since the seismic wave cannot be predicted, we select the input horizon h_v to be 1. The limitation of the control input ($u_{\max}$) is selected as $u_{\max} = 2.5 \times 10^6$ N.

Figure 4 is the results without the limitation of the control input ($u_{\max} = \infty$ N) and Fig. 5 is the results with the limitation ($u_{\max} = 2.5 \times 10^6$ N). Figure 4 shows that the MPC-based EID approach has good control performance for displacement. Figure 4 (c) shows that the control inputs of them are basically the same. However, Fig. 4 (d) shows that the MPC method modifies the EID signal at each step and it improves the control performance.

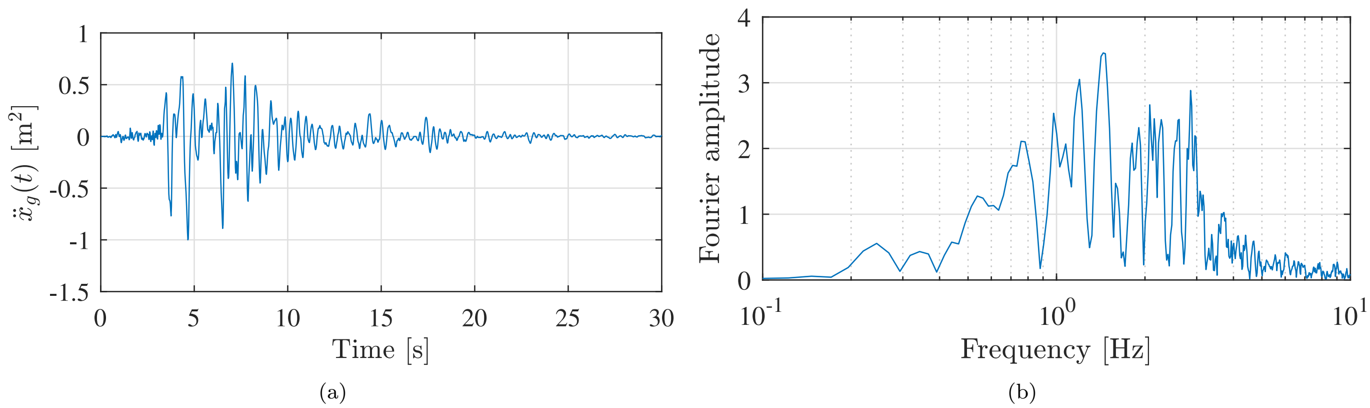

Fig. 3. Kobe wave of (a) accelerogram and (b) Fourier spectrum

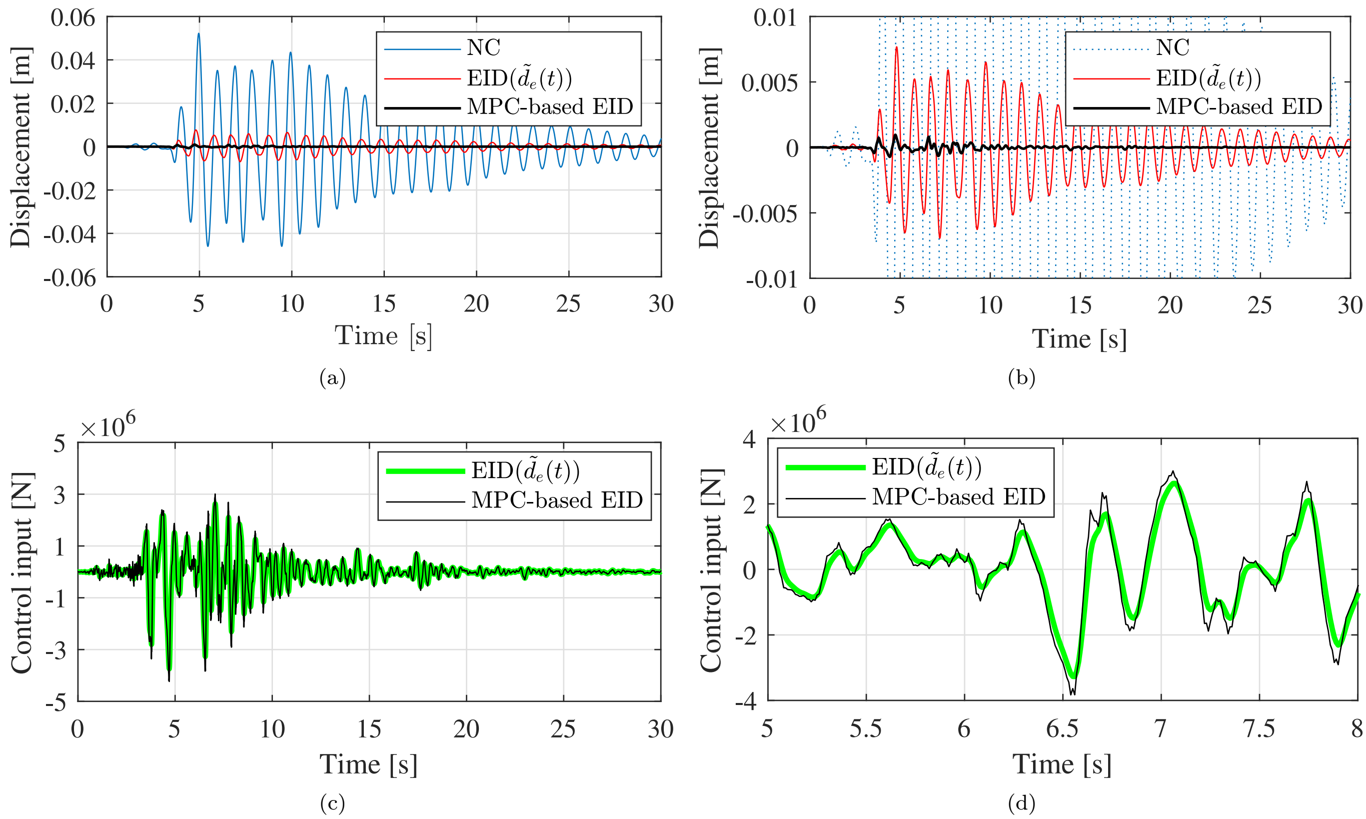

Fig. 4. Simulation result ($u_{\max} = \infty$) (a)responses for the system, (b) enrage of (a), (c) control inputs, and (d) enrage of (c)

The observer gain of the EID estimator, L, is designed by solving the following Riccati equation:

$$\begin{cases} A_c S + S A_c^{\mathrm{T}} + Q_L - S C_c R_L^{-1} C_c^{\mathrm{T}} S = 0 \\ L = S R^{-1} C_c^{\mathrm{T}} \end{cases} \tag{20}$$

where S is the solution of the Riccati equation, and Q_L (> 0) and R_L (> 0) are the weighting parameters that are selected as

$$Q_L = \begin{bmatrix} 15 & 0 \\ 0 & 15 \end{bmatrix}, \quad R_L = 0.001. \tag{21}$$

Note that we first design an observer for continues system; the observer is discretized. Then, we yield the following obserber gain:

$$L = \begin{bmatrix} 120.9 & -18.7 \\ -18.7 & 126.8 \end{bmatrix}. \tag{22}$$

Figures 5 (a) and (b) also show that the MPC method improves the control performance and the MPC-based EID approach quickly suppresses the displacement. Figures 5 (c) and (d) present that the control inputs of the two methods are almost the same if the control inputs are small (5.0 s $\sim$ 6.5 s). If the control force becomes large, the

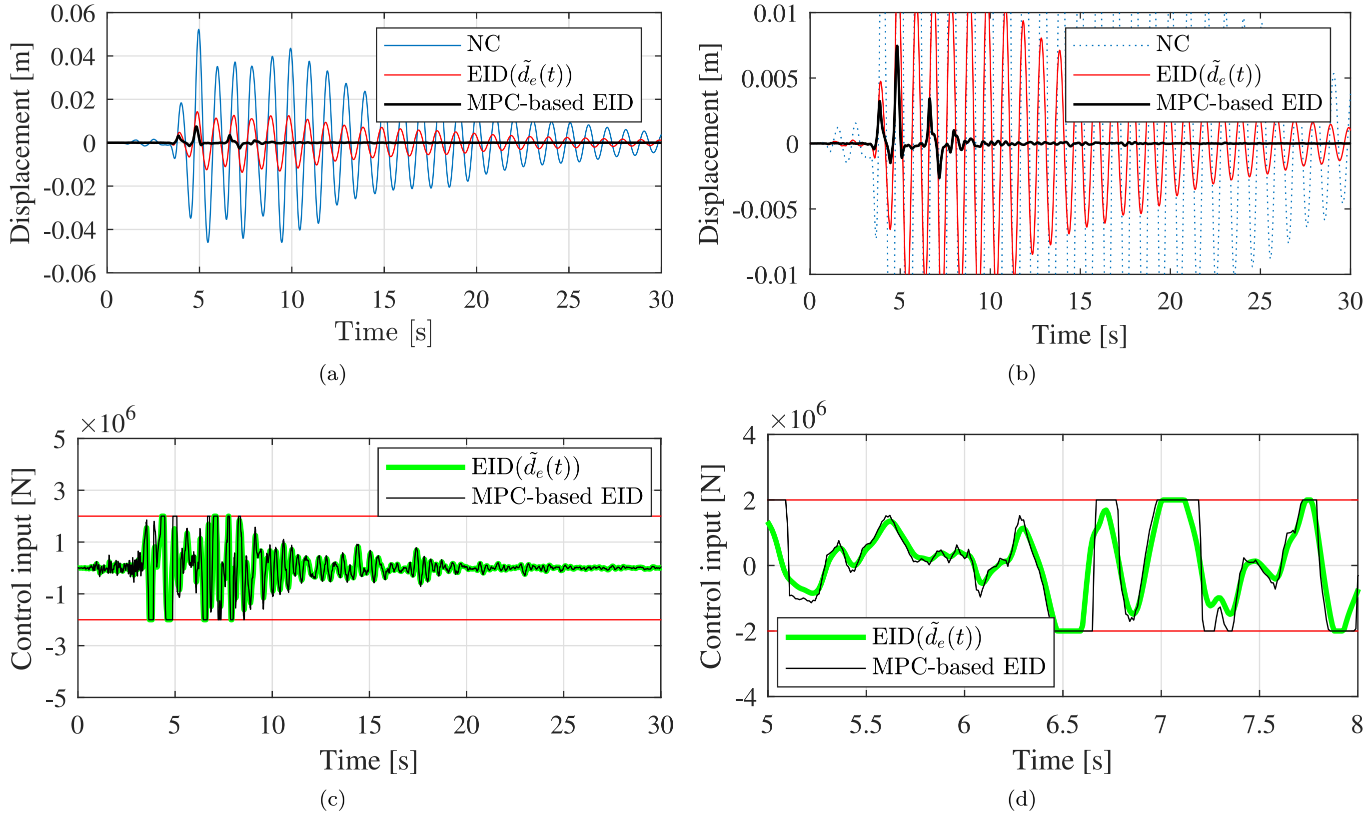

Fig. 5. Simulation result ($u_{\max} = 2.0 \times 10^6$) (a)responses for the system, (b) enrage of (a), (c) control inputs, and (d) enrage of (c)

EID $\tilde{d}_e(t)$ is saturated because it is beyond the limitation. On the other hand, the MPC method adjusts the control force so as to satisfy the limitation of the control input.

VI. Conclusions

This paper presents a new equivalent-input-disturbance (EID) approach that is combined with the MPC method, which is the MPC-based EID approach. The EID approach estimates the influence of the disturbance and rejects it. Thus, a large disturbance causes saturation of the control input, and it decreases the control performance. To solve this problem, we combine the EID approach and the model predictive control (MPC) method (MPC-based EID approach). The numerical example verifies the validity of our method.

We clarified the following points:

- The control performance of the MPC-based EID approach is better than that of the previous EID approach.
- The control input of the MPC-based EID approach is basically the same as that of the EID approach.
- However, the MPC method modifies the control input in every step, and it improves the control performance.

This study shows that the presented method has good control performance. Showing the proof of the stability for the whole of the system is one of the future works.

References

[1] J.-H. She, X. Xin, and Y. Pan “Equivalent-Input-Disturbance Approach—Analysis and Application to Disturbance Rejection in Dual-Stage Feed Drive Control System”, IEEE/ASME Transactions on Mechatronics, vol. 16 No. 2, pp. 330-340, April, 2011.

[2] K. Miyamoto, D. Sato, J. She, Y. Chen, and Q.-L. Han, ‘New spectra of responses and control force for design of equivalent-input-disturbance-based active structural control of base-isolated buildings, Journal of Sound and Vibration, vol. 507, September, 2021 (Article Numbe:116160).

[3] K. Miyamoto, J. She, J. Imani, X. Xin, and D. Sato, “Equivalent-input-disturbance approach to active structural control for seismically excited buildings”, Engineering Structures, vol. 135, pp. 392-399, October, 2016.

[4] Z. Cai, X. Lai, M. Wu, C. Lu, and L. Chen, “Equivalent-input-disturbance-based robust control of drilling trajectory with weight-on-bit uncertainty in directional drilling”, ISA Transactions, vol. 127, pp. 370-382, August, 2022.

[5] L. Jin, Y. He, C.-K. Zhang, X.-C. Shangguan, L. Jiang, and M. Wu , “Equivalent input disturbance-based load frequency control for smart grid with air conditioning loads”, Science China Information Sciences, vol. 65, January, 2022 (Article Numbe:122205).

[6] J. M. Maciejowski, “Predictive Control with Constraints”, Springer, August, 2000.

[7] T. Yu, Z. Mu, and E. A. Johnson, “Real-time neural network based semiactive model predictive control of structural vibrations”, Computers and Structures, vol. 275, January, 2023 (Article Number:106899).

[8] H. Liu, J. Yu, R. Wang, “Model predictive control of portable electronic devices under skin temperature constraints”, Energy, vol. 260, December, 2022 (Article Numbe:125185).